Reviews

Functionalized Nanoparticles and Nanostructured Surfaces for Surface-Assisted Laser Desorption/Ionization Mass Spectrometry

Ryuichi Arakawa[†] and Hideya Kawasaki

Department of Chemistry and Materials Engineering, Faculty of Chemistry, Materials and Bioengineering, Kansai University, 3-3-35 Yamate, Suita, Osaka 564–8680, Japan

Surface-assisted laser desorption/ionization time-of-flight mass spectrometry (SALDI-TOF-MS) using nanoparticles (NPs) and nanostructured surfaces as the LDI-assisting nanomaterials is a soft ionization technique that features minimal fragmentation of analytes. As compared to traditional matrix-assisted laser desorption/ionization time-of-flight mass spectrometry (MALDI-TOF-MS) using organic matrices, SALDI-MS affords several advantages, such as the ability to detect small molecules (<500 Da), easy sample preparation, low-noise background, high salt tolerance, and fast data collection without the use of an organic matrix. The performance of SALDI has been further improved recently in terms of the detection sensitivity, detection mass range from the low- to the high-mass region, a soft LDI process, the detection of both polar and nonpolar compounds, the selective detection of analytes from a complex mixture using functionalized NPs, and various applications, including imaging mass spectrometry. This review summarizes recent developments pertaining to various NPs and nanostructured surfaces for SALDI-MS.

1 Introduction

Matrix-assisted laser desorption/ionization time-of-flight mass spectrometry (MALDI-TOF-MS) using organic matrices is a soft ionization technique that features minimal fragmentation of analytes.[1,2] Using UV-absorbing organic acids, such as 2,5-dihydroxybenzoic acid (DHBA) and α-cyano-4-hydroxy-cinnamic acid (CHCA), MALDI can be used to analyze various compounds, such as polymers, peptides, and lipids. Although

Ryuichi Arakawa is Professor of Department of Chemistry and Materials Engineering, Kansai University. He received B.Sc., M.Sc., and D.Sc. degrees in analytical chemistry in 1976 from Osaka University. He has published over 200 research articles. He has also been on the editorial board of *Analytical Sciences* and *Journal of the Mass Spectrometry Society of Japan*. He received the Mass Spectrometry Society of Japan Award (2007) and the Japan Society for Analytical Chemistry Award (2009). His research interests include ionization, fragmentation, and structure determination of small molecules to supramolecular assemblies using mass spectrometry.

Hideya Kawasaki earned his BSc degree (1993) and M.Sc. (1995) from Mie University, and his D.Sc. from Kyushu University in 1998. After post-doctoral research at Kyushu University, he was an assistant Professor at Kyushu University from 1999 to 2007. He is currently an associate Professor at Kansai University. He received an incentive award (2003) from the Division of Colloid and Surface Chemistry in Chemical Society of Japan. His current research interests include the synthesis of nanoparticles with anisotropic shape or nanoclusters, and its application for analytical chemistry.

[†] To whom correspondence should be addressed.
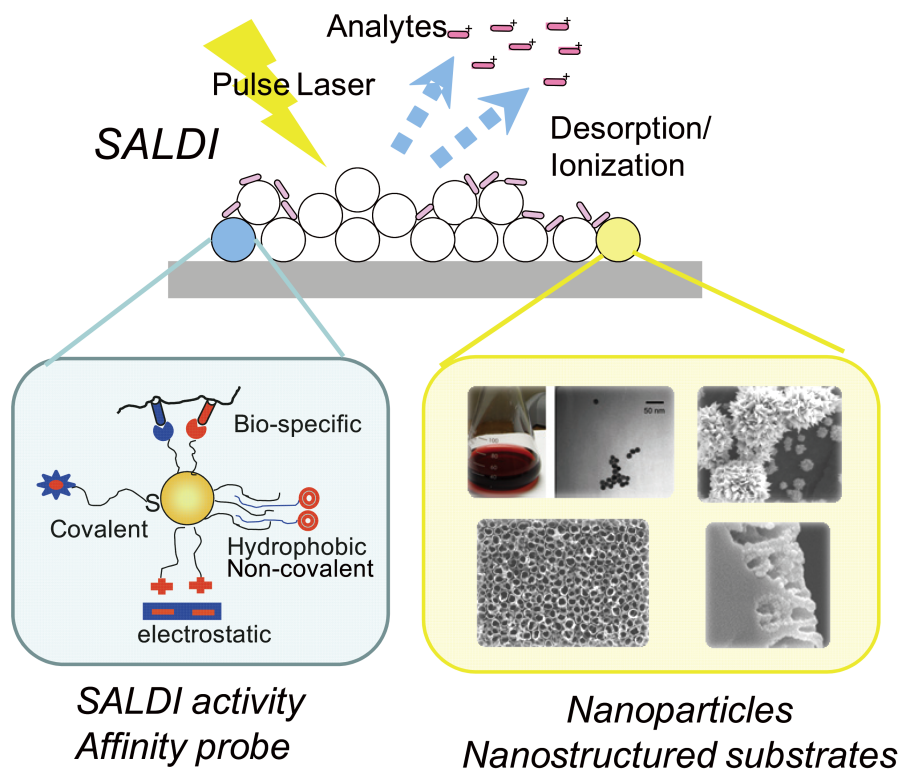E-mail: arak@kansai-u.ac.jp

Fig. 1 Schematic representations of SALDI-MS using various nanoparticles and nanostructures substrates, and an affinity probe.

MALDI-MS has been successfully used to analyze large molecules,[3-10] it has rarely been applied to low-molecular-weight compounds (<500 Da) because a large number of matrix ions appear in the low-mass range. Moreover, the suitability of different matrices for use as analyte compounds remains an empirical issue, and therefore, matrix selection and optimization of the sample preparation procedure are major issues that need to be considered carefully when employing the MALDI technique.

Various organic-matrix-free approaches to LDI-MS have been investigated in order to realize the analysis of small molecules. Surface-assisted laser desorption/ionization time-of-flight mass spectrometry (SALDI-TOF-MS) affords several advantages, such as easy sample preparation, low-noise background, high salt tolerance, and fast data collection without the use of an organic matrix. Thus, SALDI-MS serves as a promising technique for analyzing compounds in the low-mass range. The SALDI technique was originally inspired by Tanaka *et al.*, who used a suspension of cobalt nanoparticles in glycerol with a particle size of 30 nm to analyze proteins and synthetic polymers by using a pulsed UV laser.[1] Sunner referred to the use of 2- to 150-μm-sized graphite particles in glycerol solutions as a matrix as SALDI-MS,[11,12] and several groups have demonstrated the use of SALDI-MS with other inorganic particles.[13-15]

Recently, nanoparticles (NPs) and nanostructured surfaces without a liquid matrix, such as a glycerol matrix, have been utilized for SALDI-MS. Wei *et al*. have developed a matrix-free approach to LDI-MS, called desorption ionization from porous silicon (DIOS), in order to generate intact molecular ions; to do so, they used porous silicon having a large surface area with a high absorbance of UV light.[16] Because the use of organic matrices is not required, one of the most important features of DIOS is the absence of matrix interference in the low-mass

region, unlike that in MALDI. DIOS thus extends the detectable mass range of small biomolecules to less than *m/z* 500. Since then, several other types of NPs and nanostructured substrates for organic-matrix-free LDI-MS have been reported. Here, SALDI refers to the use of both NP matrices and nanostructured substrates in organic-matrix-free LDI-MS, although the meaning of the technical terms used in this field is slightly unclear.

In recent years, there has been increasing demand for high-throughput methods in the areas of drug discovery and biotechnology as well as methods for the analysis of complex mixtures in high-salt matrices and buffers; in this light, various studies have focused on, and successfully realized improvements in the performance of SALDI in terms of the detection sensitivity, detection mass range from the low- to the high-mass region, soft LDI process, detection of both polar and nonpolar compounds, selective detection of analytes from a complex mixture using functionalized NPs, and various applications including imaging mass spectrometry (IMS) (Fig. 1). Such developments in SALDI-MS have occurred in close conjunction with the fabrication of NPs and nanostructured surfaces in material chemistry and physics. A review article on SALDI-MS was reported in 2007.[17] Hence, in this paper, we mainly describe and review NPs and nanostructured surfaces developed for applications to SALDI-MS that were reported between the start of 2007 and August 2010.

2 Nanostructured Surfaces for SALDI-MS

2·1 Silicon-based substrates

Among SALDI-MS techniques employing silicon-based nanomaterials, DIOS-MS has been extensively studied. The optimal performance of DIOS is typically obtained for molecules

with weights less than 3000 Da, and thus, DIOS-MS has been developed for small-molecule detection and for the rapid detection of metabolites in biological matrices.[17,18] The surface modification of porous silicon allows DIOS-MS to be used for sample capture and enrichment in LDI-MS analysis through the analyte-specific interaction. Meng *et al*. demonstrated that the use of immobilized ligands on the porous silicon for isolating the target molecules from the background in a complex sample greatly simplified the analysis of the DIOS-MS spectra.[19] Recently, Lowe *et al*. demonstrated the combination of immunocapture with DIOS-MS using the covalent immobilization of antibodies to produce a porous immunoaffinity surface; this surface could be used for the highly selective mass spectrometric detection of illicit drugs (benzodiazepines) from a mixed analyte aqueous solution.[20] The study of interactions in protein drugs (small molecules) is very important in drug discovery. Hu *et al*. demonstrated the detection of noncovalent interactions between small molecules and proteins using DIOS-MS with chemically modified protein-terminated surfaces.[21]

In order to realize further improvements in DIOS-MS, other silicon-based nanostructured surfaces have been explored as alternatives to porous silicon; these include silicon nanowires,[22,23] nanofilament silicon with the combination of dynamic electrowetting,[24] nanostructured silicon substrates prepared by iodine-assisted etching,[25] silicon microcolumn arrays,[26] and germanium nanodots grown on a silicon wafer.[27] In addition, some commercially available SALDI substrates have been developed; as a representative example, DIOS, QuickMass consists of a nonporous germanium thin film, and nanostructured silicon-based NALDI chips.[28-30]

2·2 Signal enhancement factors on SALDI substrates

Although the SALDI mechanism, including DIOS, has not been clarified entirely, preliminary investigations indicate the signal enhancement factors for molecular ions in the SALDI mass spectra: (1) a laser-induced rapid temperature increase,[1,13,31-33] (2) porous and nanowire morphologies with a high surface area,[31,32] (3) ability to trap solvent molecules,[34,35] (4) surface functionalities, such as a terminal-OH-derived surface or hydrophobic surface,[18,23,34,36-40] (5) electrically conductive surface,[41] (6) laser-induced acoustic desorption,[42] (7) field desorption in nanowires due to laser irradiation,[22] and (8) laser-induced surface melting/restructuring.[43-45]

Among these factors, the laser-induced rapid temperature increase in the LDI substrate has been widely attributed to the thermal desorption of analyte molecules without thermal decomposition in SALDI-MS.[1,13,31-33] In such a case, the peak temperature is a function of the optical absorption coefficient, heat capacity, and heat conductivity of substrates. In particular, the high optical absorption coefficient of substrates enhances the rapid temperature increase during the LDI process, and this serves to effectively transfer energy from the surface to the analytes. Therefore, a porous silicon semiconductor with high absorption coefficients in the UV region can be used as a material for SALDI. In addition, the low thermal conductivity of porous silicon confines the heat near the surface, thus increasing the peak temperature. For example, the increased surface porosity of porous silicon is known to reduce the thermal conductivity of porous silicon (~1.2 W(m·K)), as compared to that of a single-crystalline flat silicon wafer (~130 W(m·K)).[35] In the case of a silicon nanowire, the nanowire sharply increases the surface temperature because of the 1D quantum-confined thermal energy and the decrease in the thermal conductivity of the nanowire. As a result, the use of a silicon nanowire results

in a remarkable decrease in the minimum laser irradiation energy required for analyte desorption.[23,46]

In addition to the thermal desorption process, experimental results strongly support the other contributions of a non-thermal desorption process in enhancing the ion desorption efficiency in SALDI-MS. Northen *et al*. found the correlation between the signal of the DIOS mass spectrum and the changes in the surface morphology (surface restructuring and surface melting), in which it was suggested that the desorption in DIOS is driven by surface restructuring and is not a strictly thermal process.[43] A non-thermal desorption process for laser-induced surface reconstruction/destruction has also been proposed for surface platinum melting in platinum-coated porous alumina by Wada *et al*.[44] and carbon-based substrates by Tang *et al*.[45]

The surface chemistry of LDI substrates, such as electronic surface states from dangling bonds or defects on the surface, their wettability, the interaction energy between the surface and the analyte also plays a significant role in both desorption and ionization because desorption from the analytes should involve breaking of the bond between the analytes and the surface. In the case of low wettability, a sample droplet of an aqueous solution will be localized on the SALDI plate, leading to high detection sensitivity. Chen *et al*. investigated the roles of adsorbed water, acidity, terminal OH groups, and surface morphology in SALDI of amino acids from porous graphite and silicon substrates.[34] SALDI was successfully carried out with all substrates; however, the ability to carry out SALDI was greatly reduced after the removal of physisorbed and chemisorbed water, suggesting the essential role of adsorbed water in the SALDI process.

Alimpiew *et al*. found that amorphous silicon with a high degree of surface roughness lost its LDI activity when the surface was hydrogenated.[37] They proposed the following SALDI mechanism: UV laser-induced near-surface hole trapping in a silicon substrate leads to a substantial increase in the acidity of the surface Si-OH moieties and enables proton transfer to hydrogen-bonded peptides with a high proton affinity. The thermal desorption of analyte is initiated by the UV irradiation-induced temperature increase of the surface. Yao *et al*. also suggested a similar mechanism for UV laser-induced near-surface hole trapping for a Pt-particle-deposited silicon substrate.[47]

Porous silicon surfaces are oxidized when exposed to air for extended periods; this has been reported to affect the DIOS performance.[22] Vaidyanathan *et al*. reported that surface oxidation influenced the mass spectral responses; in particular, the signal intensities of hydrophobic amino acids were noticeably reduced.[48] Liu *et al*. suggested that moderate oxidation leads to the formation of acidic Si-OH groups that benefit the analyte ionization in DIOS-MS, whereas the formation of an overoxidized silicon oxide layer reduces the overall ionization efficiency.[49]

2·3 Metal-oxide-based substrates

Along with silicon, other semiconductors with good UV absorbance are also promising candidates for SALDI-MS. As compared to silicon-based substrates, metal-oxide-based substrates afford one advantage in that they are chemically stable in air. Chen *et al*. demonstrated SALDI-MS of a titania sol-gel film.[50] A high concentration of citrate buffer was added into this system to provide the proton source and to reduce the presence of alkali cation adducts of the analytes. Surfactants, peptides, tryptic digest products, and small proteins with molecular weights below *ca*. 24 kDa, were observed in the mass spectra. Further, titania nanotube arrays (TNAs) fabricated

using anodizing processes have been developed as the substrate for SALDI-MS.[51] The background generated from TNA is very low, making this TNA substrate suitable for the analysis of small molecules, and the upper detectable mass is 29 kDa. Further, phosphopeptides can be selectively trapped on the TNA substrate by simply depositing a tryptic digest of β-casein on the titania. Yuan et al. used mesoporous tungsten titanium oxides as the substrate for the SALDI-MS of peptides.[52]

Metal-oxide nanowires with a large surface area, high photon absorption efficiency, and low heat capacity can also serve as effective SALDI substrates.[53,54] Kang et al. investigated the SALDI performance of several nanowires of oxides (ZnO and SnO₂), nitrides (GaN), and carbides (SiC) for the analysis of small molecules.[53] In the case of ZnO, the SALDI efficiency was found to be enhanced on nanowires having a length of 250 nm, corresponding to an aspect ratio of 5.

Hsu et al. demonstrated that a simple commercial Al foil could be used as a unique SALDI substrate to obtain the mass spectra of biomolecules without the need of an etching process to produce a porous surface.[42] As compared to other SALDI substrates, the use of a commercial Al foil as a substrate is the simplest and least expensive method for detecting small biomolecules.

2·4 Carbon-based substrates

Carbon-based materials have been used for SALDI-MS. The hydrophobicity of a carbon surface can change because of surface oxidation, which affects the detection sensitivity of polar and non-polar compounds. On the other hand, it should be noted that for SALDI-MS with carbon materials, an array of carbon cluster peaks, 12 m/z units apart, often appears in the low-mass region below m/z 300 at high laser fluences.

Sunner et al. first used graphite carbon dispersed in glycerol for SALDI.[11] They further developed activated carbon particles deposited on thin-layer chromatography (TLC) plates, which are suitable for both TLC functions and the SALDI process.[12] Carbon nanotubes, C70 fullerenes, and an activated carbon surface have been also reported to be effective matrices for SALDI-MS of small molecules,[55,56] peptides and proteins,[57] and steroids.[58,59]

Chen et al. first demonstrated that pencil lead is an effective SALDI matrix.[60] A silica gel surface of a TLC plate was pretreated by simply drawing a pencile line as the SALDI solid and a liquid matrix (15% sucrose/glycerol–methanol 1:1 v/v) was applied to it before sample preparation. Various groups of analytes, including methylephedrine, cytosin, PEG400, and PEG2000 can be readily ionized using a pencil lead matrix. The pencil lead matrix is an inexpensive, quick, and easy-to-use matrix. Carbon deposition using this method of pencil drawing was much more homogeneous than by applying a suspension of carbon powder mixed with a liquid matrix on the gel surface. Further, Black et al. demonstrated that analysis of a broad range of analytes including small molecules, peptides, polymers and actinides is possible using a pencil lead as a solventless matrix.[61] In practice, a 2B pencil appears to provide the optimum results.

Oxidized graphitized carbon black (GCB) particles were used as the desorption/ionization surface.[62] The surface of oxidized GCB contains more carboxylic acid groups than non-oxidized GCB; these carboxylic acid groups enhance the efficiency of the desorption/ionization process of relatively more hydrophobic compounds. Kawasaki et al. employed an oxidized, pyrolytic, highly oriented graphite polymer film with a SALDI film for an environmental analysis of low-mass analytes.[40] Several environmentally important chemicals including perfluoroalkyl-sulfonic acid, pentachlorophenol, bisphenol A, 4-hydroxy-2-

chlorobiphenyl, and benzo[a]pyrene were successfully detected by using the graphite polymer film. Recently, Dong et al. used graphene as a matrix for the analysis of low-molecular-weight compounds in SALDI-MS.[63] The use of graphene is advantageous for the analysis of polar compounds, such as amino acids, polyamines, anticancer drugs, and nucleosides as well as that of nonpolar compounds such as steroids.

2·5 Multilayer-coated substrates

Double- or multilayer-coated hybrid substrates, such as metal-coated porous alumina (platinum/alumina),[41,44] two-layered amorphous silicon,[64] titania-printed aluminum foils (titania/aluminum),[65] layer-by-layer (LBL) self-assembled films,[66,67] and DVDs coated with diamond-like carbon[68] are considered to be promising materials for SALDI-MS because the layer properties of these substances can be varied using diffrernt layer combinations. It is expected that these hybridization effects can improve the efficiency of SALDI-MS.

Okuno et al. demonsrated that platinum- or gold-coated porous alumina with sub-micrometer structures can potentially be used as a substrate for SALDI-MS of biomolecules.[41] By varying the geometries, including pore densities and diameters, Wada et al. revealed that the laser intensity required to generate ions is related to the surface porosity.[44] This double-layer-type substrate allowed the ionization of angiotensin I and verapamil at low femtomole levels. Moreover, small proteins and glycoproteins such as the 24-kDa trypsinogen and 15-kDa ribonuclease B could be ionized with sufficient sensitivity on this target.

In two-layered sample plates consisting of a substrate and a thin-film coating, Jokinen et al. demonstrated that a substrate with low thermal conductivity was superior to those with relatively higher conductivity.[64] With regard to the coating layer, an amorphous silicon coating was superior to other coatings because of its UV absorptivity and favorable surface chemistry. Good signals were obtained from the combination of a titania substrate with an amorphous silicon coating, but not from alumina-coated, silicon-nitride-coated, or uncoated sample plates.

Kawasaki et al. demonstrated that layer-by-layer (LbL) self-assembled multilayer films of AuNPs on a silicon wafer were effective SALDI substrates for the analysis of peptides and environmental pollutants.[66] The number of NP layers in LbL multilayer films had a significant effect on the LDI of angiotensin I, and the peak intensity of the peptide increased with the number of layers of AuNPs. In addition, it was found that the LbL films could be used to extract environmental pollutants (pyrene and dimethyldistearylammonium chloride) from very dilute aqueous solutions by immersing them in the sample solution. Further, the analytes trapped in the LbL film could be identified by introducing the film directly into the mass spectrometer without having to elute the analytes from the film.

3 NPs for SALDI-MS

Another approach to SALDI-MS analysis involves the use of NPs as inorganic matrices (e.g., Au, Ag, Pt, Si, SiO₂, ZnO, TiO₂, CdS, ZnS, EuF₃, and HgTe NPs). In these NPs, metal ion adductions of analytes are easily observed in the SALDI mass spectra when metal nanomaterials are used as the SALDI assisting materials.

3·1 Gold (Au) NPs

Russell's group first reported the use of size-selected AuNPs

with sizes of 2, 5, and 10 nm for SALDI-MS of peptides, where 2-nm-sized AuNPs exhibit the highest performance because of the quantum confinement effects prevalent in quantum dots.[69] The surface modification of AuNPs with 4-aminothiophenol increased the ion yields, decreased ion fragmentation, and increased the useful analyte mass range relative to citrate-capped AuNPs.[38] Anion effects on the ionization efficiency in SALDI-MS using AuNPs were also examined.[70]

Wu et al. developed protocols for sample preparation (sample-first method) with the objective of improving the shot-to-shot reproducibility of SALDI-MS using AuNPs.[71,72] AuNPs using the sample-first method offered distinctive advantages, where the sample analytes were first deposited on the plate, following which AuNPs were placed on the analytes. As compared to 2,5-DHB matrices, the analytes were detected with better shot-to-shot reproducibility in a high-salt solution and quantified even in a high-salt solution in SALDI-MS.

The optimization of the size, arrangement on the plate, and concentration of the AuNPs are important factors for effectively utilizing the Au-SALDI-MS technique. Huang et al. reported the effects of the particle sizes (14, 32, and 56 nm) and the concentrations of AuNPs on Au-SALDI-MS.[73] They found that AuNPs with a diameter of 14 nm are preferable because of the greater signal-to-noise (S/N) ratios. Tarui et al. reported SALDI-MS using nanocomposite films of cationic diblock copolymer micelles (poly(styrene-b-N-methyl-4-vinyl pyridinium iodide)) and ammonium-citrated AuNPs on silicon.[74] High ionization efficiency of peptides was realized with moderate aggregation of NPs controlled by polymer micelles on a silicon substrate.

Su et al. demonstrated the analysis of small neutral carbohydrates by SALDI-MS using bare AuNPs.[75] As compared to citrate-capped and cationic-surfactant-capped AuNPs, bare AuNPs can capture analytes on their surface; therefore, small neutral carbohydrates, which are difficult to ionized by MALDI-MS, can be cationized efficiently by SALDI-MS with AuNPs. Without derivatization, the detection limits at an S/N ratio of 3 are 82, 41, 144, and 151 nM for ribose, glucose, cellobiose, and maltose, respectively. Duan et al. found that the combination of CHCA-modified AuNPs with optimal amounts of glycerol and citric acid led to a marked improvement in peptide ionization as compared to citrate-capped or cysteamine-capped AuNPs.[76] In addition, the CHCA modification effectively suppressed the formation of Au cluster ions and analyte fragment ions, leading to cleaner mass spectra. The applicability of CHCA-AuNPs for SALDI-MS analysis of protein digests has also been demonstrated.

The quantitative determination of a variety of analytes was demonstrated by SALDI-MS using AuNPs; doing the same using MALDI-MS was found to be difficult. Chen et al. reported a method for the quantitative determination of the concentration of captopril (CAP) using N-2-mercaptopropionyl-glycine-modified AuNPs as an internal standard.[77] This approach provided linearity for CAP over the concentration range of 2.5 – 25 μM (R_2 ~0.987), with a detection limit of 1.0 μM. Chiang et al. found that mixtures of 3.5- and 14-nm-sized AuNPs allow the quantitative determination of the three aminothiols.[78] SALDI-MS provided detection limits of 2, 20, and 44 nM for glutathione, cysteine, and homocysteine, respectively.

It is well known that the excitation of surface plasmons by visible light is called localized surface plasmon resonance (LSPR). The irradiation of nanometer-sized AuNPs with visible laser light at or near the LSPR absorption band causes increased temperatures and changes in particle size.[79,80] Therefore, the use of a visible-wavelength laser in SALDI-MS of AuNPs with LSPR absorbance is expected to enhance the SALDI process of analytes.[81-85] Chen et al. reported SALDI-MS of biological molecules (peptides and carbohydrates) from Au nanorods using a Nd:YAG pulsed visible laser (532 nm).[81] Shibamoto et al. succeeded in the detection of an ultra-trace amount (of the order of several hundred zeptomoles) of sample molecules in AuNP-SALDI-MS with a visible laser (532 nm) by utilizing the effective charge interaction based on the surface plasmon excitation of AuNPs.[83]

Au nanorods have an absorption band at ~520 nm as the transverse LSPR mode and also exhibit an LSPR absorption band near the IR region. Castellana et al. demonstrated the effectiveness of the use of laser irradiation near infrared ranges with a Nd:YAG laser (1064 nm) for SALDI-MS of biomolecules using Au nanorods.[84] Gámez et al. investigated SALDI-MS with Au nanospheres, nanorods, and nanostars at four wavelengths covering the UV, visible, and near-infrared ranges.[85] A close correlation was found between the plasmonic excitation of the NPs and the LDI thresholds.

3·2 Platinum (Pt) NPs

Yonezawa et al. systematically investigated the feasibility of using various stabilizer-free bare metal (Cu, Ag, Au, and Pt) NPs for the SALDI-MS of peptides.[33] Although all metal NPs absorbed N_2 laser light (337 nm) energy in SALDI-MS, the performance of desorption/ionization of a representative peptide, angiotensin I, strongly depended on the metal element. Among these metal NPs, PtNPs exhibited the highest performance in SALDI-MS owing to their lower heat conductivity and higher melting temperature. In addition, PtNPs were stable under laser irradiation and formed few clusters. In contrast, both AgNPs and CuNPs could not detect angiotensin I by SALDI-MS. Further, surface-cleaned Pt nanomaterials with thin projections (petals) on the PtNP surface, called Pt nanoflowers, were developed for SALDI-MS of biomolecules.[86,87] SALDI-MS with Pt nanoflowers exhibited high sensitivity (of the order of a few femtomoles) for peptides and proteins with a relatively low laser energy because of thin projections on the NP surface. Chiang et al. investigated six nanomaterials (AuNPs, TiO_2 NPs, SeNPs, CdTe quantum dots (QDs), Fe_3O_4 NPs, and Pt nanosponges) for their applicability as surfaces for SALDI-MS of small analytes, peptides, and proteins.[88] Among these nanomaterials, Pt nanosponges and Fe_3O_4 NPs were the most efficient nanomaterials for proteins, with an upper detectable mass limit of ca. 25 kDa. On the other hand, AuNPs were the most effective for small analytes.

3·3 Silicon (Si) NPs

Wen et al. used SiNPs (5 – 50 nm) for SALDI-MS of small molecules.[89] Detection limits on the order of a few femtomoles per microliter were achieved for propafenone and verapamil drugs. The molecular selectivity, solvent-dependent ionization efficiency, salt tolerance, and minimal formation of salt or other adduct ions were demonstrated by using SiNPs. The further chemically modified SiNPs were found to require a very low laser fluence to induce efficient LDI through low internal energy deposition processes,[39] which is in agreement with previously reported results for silicon nanowires with the soft LDI process. "Soft" desorption with SiNPs is potentially advantageous for the analysis of labile compounds in SALDI-MS.

3·4 Metal oxide and other material based NPs

Agrawal et al. reported the analysis of peptide mixtures from urine and plasma samples with atmospheric-pressure LDI-MS
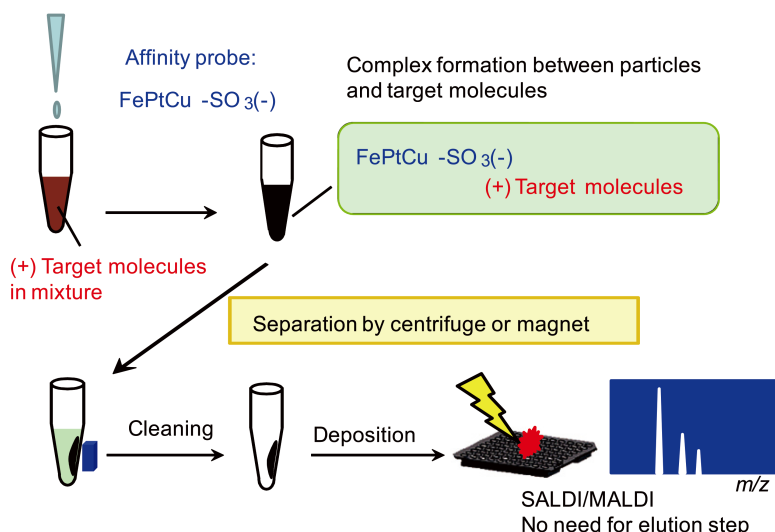
Fig. 2   Schematic of sample extraction in the case of using sulfate-modified FePtCu–SO₃(-) NPs and LDI-MS analysis.

using bare silica (SiO₂) NPs.[90]   Bare negatively charged SiO₂ NPs can be successfully utilized for the signal enhancement of peptide mixtures using electrostatic interactions between peptides and SiO₂ NPs from a dilute solution.   Recently, hydrophobic silica particles doped with carbon black have been employed for the analysis of latent fingermarks on glass and metal surfaces in order to develop a simple method for detecting nicotine and cotinine.[91]

Watanabe *et al*. have developed SALDI-MS using zinc oxide (ZnO) NPs with anisotropic shapes.[92]   ZnO-SALDI is advantageous for post-source decay (PSD) analysis and produces a simple mass spectrum in the case of phospholipids. ZnO-SALDI can be used for the analysis of synthetic polymers of polyethylene glycol (PEG), polystyrene (PS), and polymethylmethacrylate (PMMA), which had sensitivity and a molecular weight distribution comparable to that of MALDI mass spectra obtained with a DHBA matrix.

Relative to other nanomaterials commonly used for SALDI, it appears that both single-crystalline EuF₃ hexagonal microdisks and HgTe nanostructures are very effective as SALDI nanomaterials.[93,94]   Chen *et al*. reported the use of single-crystalline EuF₃ hexagonal microdisks as a background-free matrix for the analysis of small peptides and amino acids in the negative-ion reflection mode.[93]   In addition, EuF₃ microdisks were successfully used for the analysis of PEGs, and the upper limit of the detectable mass range was ~35000 Da.   It was suggested that the long-lived excited state of europium ions can transfer energy to the high-energy vibrations of an organic molecule for an effective SALDI process.   Chiang *et al*. found that HgTe nanostructures form an effective matrix for SALDI-MS of peptides and proteins.[94]   HgTe nanostructures provided relatively low background signals from metal clusters, few fragment ions, less interference from alkali-adducted analyte ions, and a high-mass range (up to 150000 Da).   The HgTe nanostructures provide detection limits of 200 pM and 14 nM for angiotensin I and bovine serum albumin, respectively, with great reproducibility (RSD: <25%).   The use of this SALDI-MS approach also enabled the detection of intact molecular ions of weak drug-protein complexes.

Finally, we comment on the surface contamination of SALDI substrates.   Because of the high surface area of NPs and

nanostructured surfaces, the surfaces of SALDI substrates can be easily contaminated when exposed to air in order; this produces strong background interferences in the mass spectra, in turn leading to obscured analyte ions in the low-mass region and suppressed ionization of larger molecules.   Sato *et al*. used surface cleaning techniques in semiconductor processing to clean a silicon-based germanium nanodot substrate for SALDI;[95] these techniques were effective in removing organic compounds and residual silver salts.   Watanabe *et al*. employed the photocatalytic surface cleaning method for amorphous TiO₂ NPs for SALDI in order to reduce the background noise and to improve the sensitivity of peptides.[96]   Recently, Law adopted an argon-plasma-etching approach to remove the surface contamination on silicon-based SALDI substrates and improve their usability.[25]

4 NPs as Affinity Probes and SALDI Matrices

For the analyses of complex biological samples, sample preparation plays a critical role in obtaining good-quality mass spectra.   In LDI-MS, including SALDI and MALDI, signal suppression from multiple components in biological samples is a significant disadvantage.   Thus, sample separation and enrichment of the analytes of interest from sample mixtures is a very important step in detecting the target analytes in LDI-MS. NPs have enormous potential for such sample pretreatments, especially for trace analyte enrichment, because the functionalization of NP surfaces with amines, carboxylic acid, thiols, epoxies, hydroxyls, and proteins enables analyte adsorption on the surface of the NPs from complex mixtures. Further, the target analytes trapped by the NPs can be identified by directly introducing the particles into the mass spectrometer for SALDI-MS analysis without the need for any further treatment (Fig. 2).

4·1 Iron-based magnetic NPs

Magnetic particles have been used for magnetic separation from complex mixtures, followed by the identification of analytes on magnetic particles by MALDI, SALDI, or Raman spectroscopy.   Titanium dioxide particles with a relatively high

specific surface area have potentially higher trapping capacities toward phosphopeptides. Chen *et al.* first developed titania-coated magnetic iron oxide NPs (Fe_3O_4@TiO_2 NPs) as an effective SALDI and affinity probe.[97] Because of their magnetic properties, the Fe_3O_4@TiO_2 NPs conjugated to the target peptides can be readily isolated from the sample solutions by employing a magnetic field. The target analytes trapped by the Fe_3O_4@TiO_2 NPs were identified by a SALDI-MS analysis. Recently, Chen *et al.* extended Fe_3O_4@TiO_2 NPs as affinity probes to concentrate and characterize pathogenic bacteria by MALDI-MS, and they demonstrated potential biomarker ions for five Gram-negative bacteria.[98] Kawasaki *et al.* used bare FePtCu NPs as magnetic NPs for SALDI-MS.[99] The fact that these bare FePtCu NPs can be modified with various functionalized thiol groups is advantageous. Sulfonate-group-modified FePtCu NPs can selectively detect lysozyme (Lyz) in human serum through the electrostatic attraction between positively charged Lyz and negatively charged FePtCu NPs.

4·2 Gold and silver NPs

Gold NPs have high affinity for thiol compounds, and hence, they can be used as affinity probes for thiol compounds. Huang *et al.* used Nile-Red-adsorbed AuNPs as selective probes and matrices for the determination of aminothiols (GSH, Cys, and HCys) through SALDI-MS.[73] SALDI-MS using AuNPs provided detection limits of 25, 54, and 34 nM for the determination of GSH, Cys, and HCys, respectively. Further, the use of aptamer-modified AuNPs (Apt-AuNPs) allowed the determination of adenosine triphosphate (ATP) with a detection limit of 0.48 μM for ATP by SALDI-MS, where the aptamers were covalently attached to the surface of AuNPs to form Apt-AuNPs that provided selectivity toward ATP.[100] McLean *et al.* demonstrated that AuNPs allowed the selective detection of phosphotyrosine in a background of phosphoserine and phosphothreonine peptides, which may be due to cation-π interactions akin to those observed between AuNPs and aromatic molecules.[69]

The use of a specific interaction, such as a silver-olefin interaction, is also attractive. Sherrod *et al.* demonstrated SALDI-MS using AgNPs to selectively ionize olefinic compounds, *e.g.*, cholesterol, 1-palmitoyl-2-oleoyl-snglycero-3-phosphocholine (POPC), and carotenoids from complex mixtures even without sample cleanup or prefractionation through the Ag-olefin interaction.[101] Chiu *et al.* applied AgNPs for the determination of three estrogens, estrone (E1), estradiol (E2), and estriol (E3), using SALDI-MS.[102] These three estrogens adsorbed weakly onto the surfaces of the AgNPs because of van der Waals forces. After centrifugation, the concentrated analytes that were adsorbed on the AgNPs were directly subjected to SALDI-MS analyses with the detection limits for E1, E2, and E3 being 2.23, 0.23, and 2.11 μM, respectively. Shrivas *et al.* presented the SALDI-MS analysis of sulfur drugs and biothiols using AgNPs capped with different functional groups without the need for further tedious separation procedures, washing steps, or elution processes.[103] Wang *et al.* analyzed aminoglycosides in human plasma samples by SALDI-MS using silver-coated AuNPs (Au@AgNPs).[104] The detection limits of aminoglycosides in plasma samples were 9, 130, 81, and 180 nM for paromomycin, kanamycin A, neomycin, and gentamicin, respectively.

4·3 Metal-oxide NPs and quantum dots

Lee *et al.* used TiO_2 NPs as selective probes and matrices for the determination of catechins using SALDI-MS.[105] The interactions between the enediol compounds and TiO_2 NPs were also evident by the change in color of the TiO_2 NP solution from milky white to orange. The detection limits for three catechins, catechin, (*S*)-epigallocatechin, and (*S*)-epigallocatechin gallate, were 0.45, 1.85, and 0.65 μM, respectively. Watanabe *et al.* demonstrated that the characteristic affinity of ZnO for amines can be utilized for amine discrimination in lipids and polymers with amine groups.[92]

Kailasa *et al.* synthesized zinc sulfide (ZnS)-semiconductor NPs capped with a variety of functional groups for the analysis of α-, β-, and γ-cyclodextrins (CDs), ubiquitin, and insulin in biological samples.[106] 3-Mercaptopropanoic acid-modified ZnS exhibited the highest efficiency toward CDs, ubiquitin, and insulin for high-sensitivity detection in SALDI-MS. The detection limits for CDs, ubiquitin, and insulin were 20 – 55, 91, and 85 nM, respectively. Further, Mn^{2+}-doped ZnS@cysteine NPs have been developed for the analysis of coccidiostats (lasalocid, monensin, salinomycin, and narasin) and peptide mixtures (Met-enk, Leu-enk, HW6, and gramicidin).[107] The doping of Mn^{2+} ions may contribute to the signal enhancement of analyte ions in the positive ion mode because of the suppression of electrons in the SALDI process.

Functionalized cadmium selenide quantum dots (CdSe QDs) with 11-mercaptoundecanoic acid have been developed for selective detection using SALDI-MS.[108] The CdSe QDs were used as preconcentrating probes for the analysis of digested peptides in lysozyme from chicken egg white by combination with microwave-assisted enzymatic digestion. As compared to MALDI, it is advantageous that the CdSe QDs exhibited high-resolution peaks for proteins in the mass spectra.

Further, in MALDI-MS, functionalized NPs have been extensively applied to isolate analytes from a complex mixture as an affinity probe; the analytes enriched on the NPs could be effectively identified by MALDI-MS with an organic matrix, such as CHCA and DHBA. The use of many NPs as affinity probes in MALDI-MS has been reported thus far: Au@magnetic particles,[109] zeolite NPs with immobilized metal ions,[110-112] diamond NPs,[113] mixed monolayer-protected AuNPs,[114] zirconium(IV)-*n*-propoxide ions,[115] Fe_3O_4@Al_2O_3 magnetic core-shell microspheres,[116-121] Fe_3O_4@ZrO_2 core-shell microspheres,[122,123] surface-modified AgNPs as a hydrophobic affinity probe,[124] gallium-oxide-coated magnetic microspheres,[125] titania,[126-128] cysteine-capped ZnSe quantum dots,[129] core-shell structure Fe_3O_4@Ta_2O_5 microspheres,[130,131] nanocrystalline titanium dioxide films,[132] multifunctional ZrO_2 NPs, and ZrO_2-SiO_2 nanorods.[133]

5 SALDI-MS for Providing Chemical Information about Surface-adsorbed Species of Nanomaterials

SALDI-MS can be a useful tool for providing chemical information about surface-adsorbed species of nanomaterials because the laser-induced desorption of analytes can preferentially occur from the surface-adsorbed species of NPs. Niidome *et al.* demonstrated that SALDI-MS can be used for analyzing adsorbates on Au nanorods. It was found that $AgBr_2^-$, which adsorbed on Au nanorod surfaces, was a key material to control the anisotropic growth of Au nanorods.[134] Chen *et al.* reported a colorimetric, label-free AuNP probe for the detection of Pb^{2+} in an aqueous solution. SALDI-MS data revealed the formation of Pb-Au alloys on the surfaces of the AuNPs in the presence of Pb^{2+} ions and 2-mercaptoethanol, which is responsible for the high-sensitive colorimetric detection of Pb^{2+}.[135] Lin *et al.* used SALDI-MS to provide strong evidence
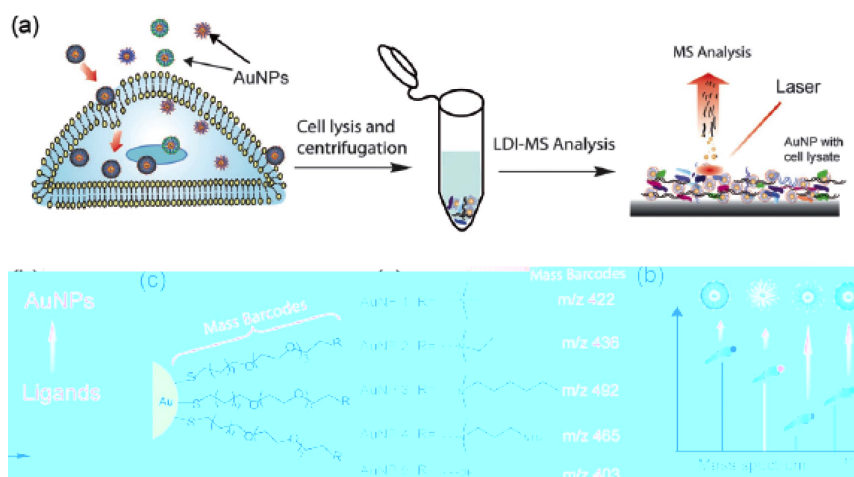
Fig. 3   Multiplexed tracking of AuNP cellular uptake by LDI-MS. (a) Schematic illustration of the analysis of the AuNPs in cell lysates by LDI-MS. (b) Illustration of an LDI mass spectrum. (c) Structural representation of the AuNPs. The mass/charge ratios (*m/z*) attached to each AuNP act as mass barcodes for identification of the AuNPs. Reprinted from Ref. 141, Copyright (2009), with permission from the RSC.

for the complex reaction of 3-mercaptopropionic acid (MPA)-modified AuNPs with analytes.[136] In the Hg^{2+}-ion-induced aggregation of MPA-AuNPs in the presence of 2,6-pyridine-dicarboxylic acid (PDCA), SALDI-MS indicated that the PDCA-Hg^{2+}-MPA coordination was responsible for the aggregation of the AuNPs.

LDI-MS has been utilized as a method for characterizing a broad range of chemical reactions of molecules attached to self-assembled monolayers (SAMs) of alkanethiolates on a gold surface, permitting the rapid characterization of the masses of alkanethiolates in the monolayer.[137] Ha *et al.* utilized SALDI-MS with cation assistance for the analysis of SAMs of alkanethiolates on gold substrates and AuNPs.[138] A simple treatment using an aqueous salt solution, such as NaI resulted in significant LDI, producing the characteristic (disulfide) ions of alkanethiolate molecules from the SAMs. This cation-assisted LDI-MS was further examined for SAMs with various terminals such as –OH, –OCH_3, –NH_2, –ethylene (–CH=CH_2), and –acetylene. Yan *et al.* demonstrated that SALDI-MS can characterize the neutral, positively, and negatively charged surface functional groups of functionalized AuNPs.[139] The gold-bound ligands are desorbed and ionized by SALDI to produce both free thiols and disulfide ions in pure and complex samples. It was also found that the semi-quantitative determination of the ligand composition of the mixed monolayer of AuNPs was possible by monitoring mixed disulfide ions in SALDI-MS.

Zhu *et al.* were the first to investigate the multiplexed analysis of AuNP uptake by cells using LDI-MS.[140,141] The cellular uptake of functionalized AuNPs with cationic or neutral surface ligands can be readily determined using the LDI-MS of cell lysates (Fig. 3). The surface ligands can be desorbed and ionized to produce both free thiols and disulfide ions from the cell to monitor the AuNPs in the cell. Using this method, it was found that subtle changes to the surface functionalities of AuNPs led to measurable changes in cellular uptake propensities.

6 SALDI-MS for Imaging Mass Spectrometry

Matrix-assisted laser desorption/ionization imaging mass

spectrometry (MALDI-IMS) has attracted considerable interest from the viewpoint of monitoring drug delivery and metabolism because it allows the simultaneous imaging of many types of metabolite molecules in tissue. Recent developments in MALDI-IMS have been published in several review articles.[142-145] However, the use of an organic matrix in MALDI-IMS can limit the spatial resolution because of the matrix crystal size, sensitivity, and detection of small compounds (<500 Da). To eliminate these problems, more recently, the SALDI technique has been applied to IMS without the use of an organic matrix.

Northen *et al.* have developed nanostructure-initiator mass spectrometry (NIMS), a tool for spatially defined IMS analysis (Fig. 4).[146] NIMS-IMS uses "initiator" molecules trapped in nanostructured surfaces or clathrates to release and ionize intact molecules adsorbed on the surface. In NIMS-IMS, tissue slices (approximately 12-μm-thick sections from a mouse embryo) are placed on the NIMS surface. Laser irradiation of the "etched" area results in the desorption/ionization of metabolites from the tissue slices placed on the NIMS surface. NIMS-IMS allows a direct characterization of peptide microarrays, direct mass analysis of single cells, tissue imaging, and direct characterization of blood and urine.[147-150] Liu *et al.* demonstrated the use of a hybrid ionization approach, matrix-enhanced surface-assisted laser desorption/ionization mass spectrometry (ME-SALDI-MS), in IMS.[151,152] In ME-SALDI, the combination of MALDI with SALDI enables the successful IMS of low-mass species with improved detection sensitivity.

As alternatives to the use of the SALDI plate, colloid dispersions, such as graphite NPs,[153-155] AgNPs,[156,157] and iron-based NPs[158,159] can be used for SALDI-IMS. In a manner similar to organic matrix applications with spray deposition, a colloidal dispersion of NPs is sprayed onto the imaging target sample. The upper layer of the sample is imaged without ion interference from below the surface of the material. Taira *et al.* found that IMS using iron-based NPs can be implemented at the cellular level because of the small NP sizes of these alternative matrices to visualize lipids and peptides at a resolution of 15 μm in mammalian tissues.[158] Rowell *et al.* reported the direct detection of drugs and their metabolites in dusted latent fingermarks by SALDI-IMS.[160] Latent fingerprint detection

(LFP) analysis was performed by a direct MS analysis of the
pre-dusted fingermarks on the surface of a target plate and,
following lifting with direct MS anaacast

8 References

1. K. Tanaka, H. Waki, Y. Ido, S. Akita, Y. Yoshida, and T. Yoshida, *Rapid Commun. Mass Spectrom.*, **1998**, *2*, 151.
2. M. Karas and nd

Commun. Mass Spectrom., **2006**, *20*, 1053; G. J. Langley, J. M. Herniman, and M. S. Townell, *Rapid Commun. Mass Spectrom.*, **2007**, *21*, 180.

62. N. Amini, M. Shariatgorji, and G. Thorsen, *J. Am. Soc. Mass Spectrom.*, **2009**, *20*, 1207.

63. X. Dong, J. Cheng, J. Li, and Y. Wang, *Anal. Chem.*, **2010**, *82*, 6208.

64. V. Jokinen, S. Aura, L. Luosujärvi, L. Sainiemi, T. Kotiaho, S. Franssila, and M. Baumann, *J. Am. Soc. Mass Spectrom.*, **2009**, *20*, 1723.

65. H. Bi, L. Qiao, J.-M. Busnel, V. Devaud, B. Liu, and H. H. Girault, *Anal. Chem.*, **2009**, *81*, 1177.

66. H. Kawasaki, T. Sugitani, T. Watanabe, T. Yonezawa, H. Moriwaki, and R. Arakawa, *Anal. Chem.*, **2008**, *80*, 7524.

67. J. Duan, M. J. Linman, and Q. Cheng, *Anal. Chem.*, **2010**, *82*, 5088.

68. M. Najam-ul-Haq, M. Rainer, C. W. Huck, P. Hausberger, H. Kraushaar, and G. K. Bonn, *Anal. Chem.*, **2008**, *80*, 7467.

69. J. A. McLean, K. A. Stumpo, and D. H. Russell, *J. Am. Chem. Soc.*, **2005**, *127*, 5304.

70. K. A. Stumpo and D. H. Russell, *J. Phys. Chem. C*, **2009**, *113*, 1642.

71. H. P. Wu, C. L. Su, H. C. Chang, and W. L. Tseng, *Anal. Chem.*, **2007**, *79*, 6215.

72. H. P. Wu, C. J. Yu, C. Y. Lin, Y. H. Lin, and W. L. Tseng, *J. Am. Soc. Mass Spectrom.*, **2009**, *20*, 875.

73. Y. F. Huang and H. T. Chang, *Anal. Chem.*, **2006**, *78*, 1485.

74. A. Tarui, H. Kawasaki, T. Taiko, T. Watanabe, T. Yonezawa, and R. Arakawa, *J. Nanosci. Nanotechnol.*, **2009**, *9*, 159.

75. C. L. Su and W. L. Tseng, *Anal. Chem.*, **2007**, *79*, 1626.

76. J. Duan, M. J. Linman, C. Y. Chen, and Q. J. Cheng, *J. Am. Soc. Mass Spectrom.*, **2009**, *20*, 1530.

77. W. T. Chen, C. K. Chiang, Y. W. Lin, and H. T. Chang, *J. Am. Soc. Mass Spectrom.*, **2010**, *21*, 864.

78. N. C. Chiang, C. K. Chiang, Z. H. Lin, T. C. Chiu, and H. T. Chang, *Rapid Commun. Mass Spectrom.*, **2009**, *23*, 3063.

79. S. Link, C. Burda, M. B. Mohamed, B. Nikoobakht, and M. A. El-Sayed, *J. Phys. Chem. A*, **1999**, *103*, 1165.

80. H. Kurita, A. Takami, and S. Koda, *Appl. Phys. Lett.*, **1998**, *72*, 789.

81. L. C. Chen, J. Yonehama, T. Ueda, H. Hori, and K. Hiraoka, *J. Mass Spectrom.*, **2007**, *42*, 346.

82. M. T. Spencer, H. Furutani, S. J. Oldenburg, T. K. Darlington, and K. A. Prather, *J. Phys. Chem. C*, **2008**, *112*, 4083.

83. K. Shibamoto, K. Sakata, K. Nagoshi, and T. Korenaga, *J. Phys. Chem. C*, **2009**, *113*, 17774.

84. E. T. Castellana, R. C. Gamez, M. E. Gomez, and D. H. Russell, *Langmuir*, **2010**, *26(8)*, 6066.

85. F. Gámez, P. Hurtado, P. M. Castillo, C. Caro, A. R. Hortal, P. Zaderenko, and B. Martínez-Haya, *Plasmonics*, **2010**, *5*, 125.

86. H. Kawasaki, T. Yonezawa, T. Watanabe, and R. Arakawa, *J. Phys. Chem. C*, **2007**, *111*, 16278.

87. H. Kawasaki, T. Yao, T. Suganuma, K. Okumura, Y. Iwaki, T. Yonezawa, T. Kikuchi, and R. Arakawa, *Chem.—Eur. J.*, **2010**, *16*, 10832.

88. C. K. Chiang, N. C. Chiang, Z. H. Lin, G. Y. Lan, Y. W. Lin, and H. T. Chang, *J. Am. Soc. Mass Spectrom.*, **2010**, *21*, 1204.

89. X. Wen, S. Dagan, and V. H. Wysocki, *Anal. Chem.*, **2007**, *79*, 434.

90. K. Agrawal and H. F. Wu, *Rapid Commun. Mass Spectrom.*, **2008**, *22*, 283.

91. M. Benton, F. Rowell, L. Sundard, and M. Janc, *Surf. Interface Anal.*, **2010**, *42*, 378.

92. T. Watanabe, H. Kawasaki, T. Yonezawa, and R. Arakawa, *J. Mass Spectrom.*, **2008**, *43*, 1063.

93. Z. Chen, Z. Geng, D. Shao, Y. Mei, and Z. Wang, *Anal. Chem.*, **2009**, *81*, 7625.

94. C. K. Chiang, Z. Yang, Y. W. Lin, W. T. Chen, H. J. Lin, and H. T. Chang, *Anal. Chem.*, **2010**, *82*, 4543.

95. H. Sato, A. Nemoto, A. Yamamoto, and H. Tao, *Rapid Commun. Mass Spectrom.*, **2009**, *23*, 603.

96. T. Watanabe, K. Okumura, H. Kawasaki, and R. Arakawa, *J. Mass. Spectrom.*, **2009**, *44*, 1443.

97. C. T. Chen and Y. C. Chen, *Anal. Chem.*, **2005**, *77*, 5912.

98. W. J. Chen, P. J. Tsai, and Y. C. Chen, *Anal. Chem.*, **2008**, *80*, 9612.

99. H. Kawasaki, T. Akira, T. Watanabe, K. Nozaki, T. Yonezawa, and R. Arakawa, *Anal. Bioanal. Chem.*, **2009**, *395*, 1423.

100. Y. F. Huang and H. T. Chang, *Anal. Chem.*, **2007**, *79*, 4852.

101. S. D. Sherrod, A. J. Diaz, W. K. Russell, P. S. Cremer, and D. H. Russell, *Anal. Chem.*, **2008**, *80*, 6796.

102. T. C. Chiu, L. C. Chang, C. K. Chiang, and H. T. Chang, *J. Am. Soc. Mass Spectrom.*, **2008**, *19*, 1343.

103. K. Shrivas and H. F. Wu, *Rapid Commun. Mass Spectrom.*, **2008**, *22*, 2863.

104. M. T. Wang, M. H. Liu, R. C. Wang, and S. Y. Changa, *J. Am. Soc. Mass Spectrom.*, **2009**, *20*, 1925.

105. K. H. Lee, C. K. Chiang, Z. H. Lin, and H. T. Chang, *Rapid Commun. Mass Spectrom.*, **2007**, *21*, 2023.

106. S. K. Kailasa, K. Kiran, and H. F. Wu, *Anal. Chem.*, **2008**, *80*, 9681.

107. S. K. Kailasaab and H. F. Wu, *Analyst*, **2010**, *135*, 1115.

108. K. Shrivas, S. K. Kailasa, and H. F. Wu, *Proteomics*, **2009**, *9*, 2656.

109. C. H. Teng, K. C. Ho, Y. S. Lin, and Y. C. Chen, *Anal. Chem.*, **2004**, *76*, 4337.

110. Y. Zhang, X. Yu, X. Wang, W. Shan, P. Yang, and Y. Tang, *Chem. Commun.*, **2004**, 2882.

111. Y. Zhang, X. Wang, W. Shan, B. Wu, H. Fan, X. Yu, Y. Tang, and P. Yang, *Angew. Chem., Int. Ed.*, **2005**, *44*, 615.

112. Y. Komori, H. Shima, T. Fujino, J. N. Kondo, K. Hashimoto, and T. Korenaga, *J. Phys. Chem. C*, **2010**, *114*, 1593.

113. X. L. Kong, L. C. L. Huang, C. M. Hsu, W. H. Chen, C. C. Han, and H. C. Chang, *Anal. Chem.*, **2005**, *77*, 259.

114. B. N. Y. Vanderpuije, G. Han, V. M. Rotello, and R. W. Vachet, *Anal. Chem.*, **2006**, *78*, 5491.

115. G. R. Blacken, M. Volný, T. Vaisar, M. Sadílek, and F. Tureek, *Anal. Chem.*, **2007**, *79*, 5449.

116. C. T. Chen, W. Y. Chen, P. J. Tsai, K. Y. Chien, J. S. Yu, and Y. C. Chen, *J. Proteome Res.*, **2007**, *6*, 316.

117. Y. Li, Y. Liu, J. Tang, H. Lin, N. Yao, X. Shen, C. Denga, P. Yang, and X. Zhang, *J. Chromatogr., A*, **2007**, *1172*, 57.

118. P. C. Lin, M. C. Tseng, A. K. Su, Y.-J. Chen, and C. C. Lin, *Anal. Chem.*, **2007**, *79*, 3401.

119. J. C. Liu, P. J. Tsai, Y. C. Lee, and Y. C. Chen, *Anal. Chem.*, **2008**, *80*, 5425.

120. C. T. Chen and Y. C. Chen, *J. Biomed. Nanotechnol.*, **2008**, *4*, 73.

121. C. T. Chen and Y. C. Chen, *J. Mass Spectrom.*, **2008**, *43*, 538.

122. Y. Li, T. Leng, H. Lin, C. Deng, X. Xu, N. Yao, P. Yang, and X. Zhang, *J. Proteome Res.*, **2007**, *6*, 4498.

123. C. Y. Lo, W. Y. Chen, C. T. Chen, and Y. C. Chen, *J. Proteome Res.*, **2007**, *6*, 887.

124. K. Shrivas and H. F. Wu, *Anal. Chem.*, **2008**, *80*, 2583.

125. Y. Li, H. Lin, C. Deng, P. Yang, and X. Zhang, *Proteomics*, **2008**, *8*, 238.

126. C. T. Chen and Y. C. Chen, *Anal. Chem.*, **2004**, *76*, 1453.

127. P. Lorkiewicz and M. C. Yappert, *Anal. Chem.*, **2009**, *81*, 6596.

128. N. Hasan, H.-F. Wu, Y.-H. Li, and M. Nawaz, *Anal. Bioanal. Chem.*, **2010**, *396*, 2909.

129. L. A. Shastri, S. K. Kailasa, and H. F. Wu, *Rapid Commun. Mass Spectrom.*, **2009**, *23*, 2247.

130. H. Y. Lin, W. Y. Chen, and Y. C. Chen, *Anal Bioanal. Chem.*, **2009**, *394*, 2129.

131. D. Qi, J. Lu, C. Deng, and X. Zhang, *J. Chromatogr., A*, **2009**, *1216*, 5533.

132. M.-L. Niklew, U. Hochkirch, A. Melikyan, T. Moritz, S. Kurzawski, H. Schlter, I. Ebner, and M. W. Linscheid, *Anal. Chem.*, **2010**, *82*, 1047.

133. S. K. Kailasa and H.-F. Wu, *Anal. Bioanal. Chem.*, **2010**, *396*, 1115.

134. Y. Niidome, Y. Nakamura, K. Honda, Y. Akiyama, K. Nishioka, H. Kawasaki, and N. Nakashima, *Chem. Commun.*, **2009**, 1754.

135. Y. Y. Chen, H. T. Chang, Y. C. Shiang, Y. L. Hung, C. K. Chiang, and C. C. Huang, *Anal. Chem.*, **2009**, *81*, 9433.

136. Y. W. Lin, W. T. Chen, and H. T. Chang, *Rapid Commun. Mass Spectrom.*, **2010**, *24*, 933.

137. M. Mrksich, *ACS Nano*, **2008**, *1*, 7.

138. T. K. Ha, T. G. Lee, N. W. Song, D. W. Moon, and S. Y. Han, *Anal. Chem.*, **2008**, *80*, 8526.

139. B. Yan, Z. J. Zhu, O. R. Miranda, A. Chompoosor, V. M. Rotello, and R. W. Vachet, *Anal. Bioanal. Chem.*, **2010**, *396*, 1025.

140. Z. J. Zhu, P. S. Ghosh, O. R. Miranda, R. W. Vachet, and V. M. Rotello, *J. Am. Chem. Soc.*, **2008**, *130*, 14139.

141. Z. J. Zhu, V. M. Rotello, and R. W. Vachet, *Analyst*, **2009**, *134*, 2183.

142. Y. Sugiura and M. Setou, *J. Neuroimmune Pharmacol.*, **2010**, *5*, 31.

143. K. Chughtai and R. M. A. Heeren, *Chem. Rev.*, **2010**, *110*, 3237.

144. A. Svatoš, *Trends Biotechnol.*, **2010**, *28*, 425.

145. R. J. A. Goodwin and A. R Pitt, *Bioanalysis*, **2010**, *2(2)*, 279.

146. T. R. Northen, O. Yanes, M. T. Northen, D. Marrinucci, W. Uritboonthai, J. Apon, S. L. Golledge, A. Nordström, and G. Siuzdak, *Nature*, **2007**, *449*, 1033.

147. H.-K. Woo, T. R. Northen, O. Yanes, and G. Siuzdak, *Nat. Protoc.*, **2008**, *3*, 1341.

148. W. Reindl and T. R. Northen, *Anal. Chem.*, **2010**, *82*, 3751.

149. O. Yanes, H.-K. Woo, T. R. Northen, S. R. Oppenheimer, L. Shriver, J. Apon, M. N. Estrada, M. J. Potchoiba, R. Steenwyk, M. Manchester, and G. Siuzdak, *Anal. Chem.*, **2009**, *81*, 2969.

150. G. J. Patti, H.-K. Woo, O. Yanes, L. Shriver, D. Thomas, W. Uritboonthai, J. V. Apon, R. Steenwyk, M. Manchester, and G. Siuzdak, *Anal. Chem.*, **2010**, *82*, 121.

151. Q. Liu, Y. Xiao, C. Pagan-Miranda, Y. M. Chiu, and L. He, *J. Am. Soc. Mass Spectrom.*, **2009**, *20*, 80.

152. Q. Liu and L. He, *J. Am. Soc. Mass Spectrom.*, **2009**, *20*, 2229.

153. S. Cha and E. S. Yeung, *Anal. Chem.*, **2007**, *79*, 2373.

154. H. Zhang, S. Cha, and E. S. Yeung, *Anal. Chem.*, **2007**, *79*, 6575.

155. S. Cha, H. Zhang, H. I. Ilarslan, E. S. Wurtele, L. Brachova, B. J. Nikolau, and E. S. Yeung, *Plant J.*, **2008**, *55*, 348.

156. T. Hayasaka, N. Goto-Inoue, N. Zaima, K. Shrivas, Y. Kashiwagi, M. Yamamoto, M. Nakamoto, and M. Setou, *J. Am. Soc. Mass Spectrom.*, **2010**, *21*, 1446.

157. S. Cha, Z. Song, B. J. Nikolau, and E. S. Yeung, *Anal. Chem.*, **2009**, *81*, 2991.

158. S. Taira, Y. Sugiura, S. Moritake, S. Shimma, Y. Ichiyanagi, and M. Setou, *Anal. Chem.*, **2008**, *80*, 4761.

159. H. Ageta, S. Asai, Y. Sugiura, N. Goto-Inoue, N. Zaima, and M. Setou, *Med. Mol. Morphol.*, **2009**, *42*, 16.

160. F. Rowell, K. Hudson, and J. Seviour, *Analyst*, **2009**, *134*, 701.

161. H. W. Tang, W. Lu, C. M. Che, and K. M. Ng, *Anal. Chem.*, **2010**, *82*, 1589.

162. K. Aguilar-Arteaga, J. A. Rodriguez, and E. Barrado, *Anal. Chim. Acta*, **2010**, *674*, 157.

163. J. A. Bradshaw, O. S. Ovchinnikova, K. A. Meyer, and D. E. Goeringer, *Rapid Commun. Mass Spectrom.*, **2009**, *23*, 3781.

164. S. Alimpiev, A. Grechnikov, J. Sunner, A. Borodkov, V. Karavanskii, Ya. Simanovsky, and S. Nikiforov, *Anal. Chem.*, **2009**, *81*, 1255.

165. N. Amini, M. Shariatgorji, C. Crescenzi, and G. Thorsén, *Anal. Chem.*, **2010**, *82*, 290.

166. D. Nedelkov and R. W. Nelson, *Trends Biotechnol.*, **2003**, *21*, 301.

167. D. Nedelkov, *Anal. Chem.*, **2007**, *79*, 5987.

168. A. Madeira, E. Öhman, A. Nilsson, B. Sjögren, P. E. Andrén, and P. Svenningsson, *Nat. Protoc.*, **2009**, *4*, 1023.

169. E. Ohman, A. Nilsson, A. Madeira, B. Sjögren, P. E. Andrén, and P. Svenningsson, *J. Proteome Res.*, **2008**, *7*, 5333.

170. J. N. Anker, W. Paige Hall, M. P. Lambert, P. T. Velasco, M. Mrksich, W. L. Klein, and R. P. Van Duyne, *J. Phys. Chem. C*, **2009**, *113(15)*, 5891.

171. K. P. Law and J. R. Larkin, *Anal. Bioanal. Chem.*, DOI 10.1007/s00216-010-4063-3.